



# Density jump for parallel and perpendicular collisionless shocks

Antoine Bret<sup>1,2</sup>  and Ramesh Narayan<sup>3</sup> 

<sup>1</sup>ETSI Industriales, Universidad de Castilla-La Mancha, 13071 Ciudad Real, Spain; <sup>2</sup>Instituto de Investigaciones Energéticas y Aplicaciones Industriales, Campus Universitario de Ciudad Real, 13071 Ciudad Real, Spain and <sup>3</sup>Harvard-Smithsonian Center for Astrophysics, 60 Garden Street, Cambridge, MA 02138, USA

## Research Article

**Cite this article:** Bret A, Narayan R (2020). Density jump for parallel and perpendicular collisionless shocks. *Laser and Particle Beams* **38**, 114–120. <https://doi.org/10.1017/S0263034620000117>

Received: 10 February 2020  
Accepted: 6 March 2020  
First published online: 14 April 2020

### Keywords:

Collisionless shocks; magnetohydrodynamics; plasma instabilities; Rankine–Hugoniot

### Author for correspondence:

Antoine Bret, Universidad de Castilla-La Mancha, ETSI INDUSTRIALES, Avda Camilo José Cela s/n, 13071 Ciudad Real, Spain.  
E-mail: [antoineclaude.bret@uclm.es](mailto:antoineclaude.bret@uclm.es)

### Abstract

In a collisionless shock, there are no binary collisions to isotropize the flow. It is therefore reasonable to ask to which extent the magnetohydrodynamics (MHD) jump conditions apply. Following up on recent works which found a significant departure from MHD in the case of parallel collisionless shocks, we here present a model allowing to compute the density jump for collisionless shocks. Because the departure from MHD eventually stems from a sustained downstream anisotropy that the Vlasov equation alone cannot specify, we hypothesize a kinetic history for the plasma, as it crosses the shock front. For simplicity, we deal with non-relativistic pair plasmas. We treat the cases of parallel and perpendicular shocks. Non-MHD behavior is more pronounced for the parallel case where, according to MHD, the field should not affect the shock at all.

## Introduction

Collisionless shocks are shockwaves that can be sustained in diluted plasmas through collective plasma phenomena (Sagdeev, 1966). As a result, their front can be several orders of magnitude shorter than the mean free path for close binary collisions. A good example is the bow shock of the earth magnetosphere in the solar wind in which front is about 100 km thick, while the proton mean free path at the same location is of the order of the Sun–Earth distance (Bale *et al.*, 2003; Schwartz *et al.*, 2011). In the absence of collisions to isotropize the flow, it is reasonable to ask to which extent magnetohydrodynamics (MHD) jump conditions still apply to collisionless shocks.

In a series of recent works on collisionless shocks in pair plasmas, it was found that a flow-aligned field can precisely hinder the isotropization of the downstream so that the density jump becomes a function of the field (Bret, 2016; Bret *et al.*, 2017a, 2017b; Bret and Narayan, 2018). This stands in contrast with the MHD result where a parallel shock is independent of the field (Lichnerowicz, 1976).

The goal of the present paper is to devise a theory of the density jump in the collisionless case, accounting for a field parallel or perpendicular to the front. The departure from the MHD jump is eventually related to pressure anisotropy. In this respect, it is well known that ions and electrons exhibit different temperatures in electron/ion shocks (Tidman, 1967; Zel'dovich and Raizer, 2002; Guo *et al.*, 2017, 2018; Miceli *et al.*, 2019). This is why we chose pair plasmas for a start, where each species has the same temperatures. Dealing with the anisotropy can then be achieved, considering two temperature parameters instead of four.

Although the simulations performed in Bret *et al.* (2017b) showing the departure from MHD behavior were relativistic, we here study the non-relativistic regime for simplicity.

Some authors already derived the MHD equations in the presence of a pressure anisotropy (Karimabadi *et al.*, 1995; Vogl *et al.*, 2001; Gerbig and Schlickeiser, 2011). Yet, the degree of anisotropy is treated as a free parameter in these references. Here, we compute it for the case of an isotropic upstream.

Since the departure from MHD prescriptions can be traced back to a downstream anisotropy, a first thought could be to compute it from the Vlasov equation. Yet, it is well known that a Vlasov plasma in the presence of an external magnetic field offers a range of *stable* anisotropies (Gary, 1993). This has been nicely confirmed by the *in situ* analysis of the solar wind (Bale *et al.*, 2009; Maruca *et al.*, 2011; Schlickeiser *et al.*, 2011). The problem of the determination of the downstream state is therefore underdetermined. This is why we resort to a hypothesis on the kinetic history of the plasma as it crosses the front.

As pictured in Figure 1, we assume that the upstream of the shock is isotropic and then comes the main assumption of this work as it crosses the front, the temperature  $T_{\perp}$  perpendicular to the flow, here  $T_y$ , is conserved. This can be justified in the strong-field regime (Larmor radius  $\ll$  other dimensions) through the “double adiabatic” approximation (Chew *et al.*, 1956). As we shall see, this assumption, coupled with the conservation equations, suffices to determine all downstream quantities.

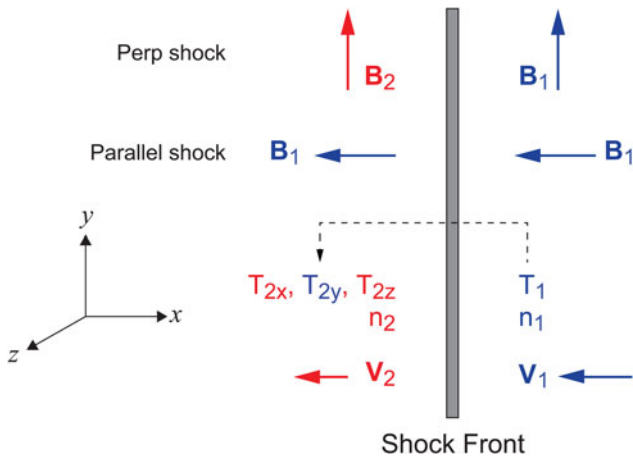


**Fig. 1.** System considered. The plasma goes from right, subscripts “1”, to left, subscripts “2”. For the parallel case, the field is the same on both sides of the front. For the perpendicular case, there is a jump in the field. In both cases, we assume that the downstream plasma goes through a stage with  $T_{2y} = T_1$ .

This stage where the downstream plasma  $T_{2y}$  inherits its upstream value is called “Stage 1”. It can be stable or unstable. If the field is too weak, “Stage 1” will generally be unstable. The plasma will then move to “Stage 2”, on the nearest stability threshold (not the same, depending on the orientation of the field). Here again, imposing a threshold condition, together with the conservation equations, allows for a full determination of this “Stage 2”.

We eventually come up with a full determination of the downstream anisotropy in terms of the field. At low magnetization, it will be given by Stage 2 because Stage 1 is unstable. Then, for high enough a field, Stage 1 is stable and determines the state of the downstream.

Since we deal with Vlasov plasmas, the temperatures in the directions perpendicular to the field must be equal (see Landau and Lifshitz, 1981, §53). Hence,

- For the parallel case,  $T_{2y} = T_1$  implies also  $T_{2z} = T_1$  since the field is along the  $x$ -axis.
- For the perpendicular case, we have  $T_{2x} = T_{2z}$  since the field is along the  $y$ -axis.

**Dimensionless parameters**

*Measuring the field:* In the collisionless shocks literature, especially the one devoted to the particle-in-cell simulation of such shocks (Sironi and Spitkovsky, 2009; Niemiec *et al.*, 2012; Plotnikov *et al.*, 2018), the field is frequently measured by the  $\sigma$  parameter,

$$\sigma = \frac{B_1^2/4\pi}{n_1 V_1^2}, \tag{1}$$

measuring the ratio of the upstream magnetic energy to the upstream kinetic energy. Yet, in the kinetic instabilities literature (Gary, 1993), the field is rather measured in terms of the  $\beta_{\parallel}$  parameter,  $\beta_{\parallel} = nT_{\parallel}/B^2/8\pi$ , where  $\parallel$  refers to the direction parallel to the field. Since the stability issue here is related to the downstream plasma, we define

$$\beta_{2\parallel} = \frac{n_2 T_{2\parallel}}{B_2^2/8\pi}. \tag{2}$$

When dealing with the parallel shock case, we shall set  $T_{2\parallel} = T_{2x}$ . And when dealing with the perpendicular shock case, we shall set  $T_{2\parallel} = T_{2y}$ .

*Mach number* In shock physics, it is usual to define an upstream Mach number as  $\mathcal{M}_1^2 = n_1 V_1^2/\gamma P_1$ , where  $\gamma$  is the adiabatic index of the fluid. Yet, the present model constrains the degrees of freedom of the plasma when “freezing” some temperatures at the front crossing. It is therefore preferable to define the following pseudo-Mach number, which allows for a unified description of all the cases treated in the sequel,

$$\chi_1^2 = \frac{V_1^2}{P_1/n_1}. \tag{3}$$

Finally, we define the density jump parameter  $r$  as

$$r = \frac{n_2}{n_1} \tag{4}$$

and the downstream anisotropy parameter  $A_2$  as

$$A_2 = \frac{T_{2\perp}}{T_{2\parallel}}, \tag{5}$$

where again  $\parallel$  and  $\perp$  are with respect to the field. When dealing with the parallel shock case, we shall set  $A_2 = T_{2y,z}/T_{2x}$ . And when dealing with the perpendicular shock case, we shall set  $A_2 = T_{2x,z}/T_{2y}$ .

**Parallel case**

This setup is especially relevant to study departures from MHD behavior since for a parallel shock, the MHD conclusion is that the fluid and the field are disconnected. In other words, the shock does not depend on the field. Therefore, any departure from the field-free jump must be related to a departure from MHD. The jump equations for the present case are (Kulsrud, 2005)

$$n_1 V_1 = n_2 V_2, \tag{6}$$

$$n_1 V_1^2 + P_1 = n_2 V_2^2 + P_{2x}, \tag{7}$$

$$\frac{V_1^2}{2} + \frac{P_1}{n_1} + U_1 = \frac{V_2^2}{2} + U_2 + \frac{P_{2x}}{n_2}, \tag{8}$$

where the external magnetic field does not appear and  $U_i$  is the internal energy. Note that the pressure component for the anisotropic downstream is  $P_{2x}$ , the one along the  $x$ -axis, since this is the direction where the fluid is pushed (Feynman *et al.*, 1963, §40–3). We shall now solve this system imposing  $T_{\perp}$  conservation, that is Stage 1. We shall then assess the stability of this stage before computing the properties of Stage 2, in case Stage 1 is unstable.

**Stage 1 density jump and anisotropy**

The constraint  $T_{1\perp} = T_1$  is introduced through the expression of the internal energy  $U_2$ . In an isotropic fluid, we would have  $U = (\sum P_i)/2n = \frac{3}{2}nP$  (for an adiabatic index  $\gamma = 5/3$ ). In the present case, we write  $U_2 = (P_{2x} + P_{2y} + P_{2z})/2n_2 = (P_{2x} + 2P_{2y})/2n_2$ . We then write  $P_{2y} = n_2 k_B T_{2y}$  and use our assumption of the

conservation of  $T_{\perp}$ , that is,  $T_y$ , to write  $P_{2y} = n_2 k_B T_1$ . We finally obtain

$$U_2 = \frac{1}{2n_2} (P_{2x} + 2n_2 k_B T_1) = \frac{P_{2x}}{2n_2} + \frac{P_1}{n_1}. \tag{9}$$

From there, the system (6)–(8) can be solved as follows: we first use Eq. (6) to eliminate  $V_2$  from the other equations. Then, we replace  $U_2$  in (8) by its expression above and eliminate  $P_{2x}$  between (7) and (8) to obtain an equation for  $n_2$ . The result is

$$\frac{n_2}{n_1} = r = \frac{2\chi_1^2}{3 + \chi_1^2}. \tag{10}$$

The jump so defined goes to unity for  $\chi_1 = \sqrt{3}$  so that smaller values are unphysical. Also, it goes to 2 in the strong shock limit  $\chi_1 \gg 1$ , which is the jump for a non-relativistic 1D gas.

The anisotropy  $A_2$  can now be computed from

$$A_2 = \frac{T_{2\perp}}{T_{2\parallel}} = \frac{T_{2y,z}}{T_{2x}} = \frac{T_1}{T_{2x}} = \frac{P_1/n_1}{P_{2x}/n_2}. \tag{11}$$

Inserting the expression (10) for  $n_2$  in one of the two equations previously derived for  $P_{2x}$ , the equation above allows to derive the anisotropy. The result is

$$A_2 = \frac{4\chi_1^2}{\chi_1^4 + 2\chi_1^2 - 3}. \tag{12}$$

This quantity is smaller than 1 for  $\chi_1 > \sqrt{3}$ . Therefore, within the physical limits of the present model,  $A_2 < 1$ .

**Stage 1 stability**

The conservation of  $T_{\perp}$  at the front crossing leads therefore to the jump (10) with the anisotropy (12). In electron/ion plasmas, the main instabilities are the firehose and the mirror instabilities. They are retrieved in pair plasmas, with the same stability thresholds (Gary and Karimabadi, 2009).

The stability diagram formed by these instabilities is pictured in Figure 2 in the  $(\beta_{2\parallel}, T_{2\perp}/T_{2\parallel} = A_2)$  phase space. For  $A_2 < 1$ , the plasma can be firehose unstable, with a threshold found for

$$\frac{T_{2\perp}}{T_{2\parallel}} = 1 - \frac{1}{\beta_{2\parallel}}. \tag{13}$$

For  $A_2 > 1$ , the plasma can be mirror unstable, with a threshold found for

$$\frac{T_{2\perp}}{T_{2\parallel}} = 1 + \frac{1}{\beta_{2\parallel}}. \tag{14}$$

We deal here with the parallel case and just checked from Eq. (12) that  $A_2 < 1$ . Stage 1 may therefore be firehose unstable if  $A_2 < 1 - 1/\beta_{2\parallel}$ . The parameter  $\beta_{2\parallel}$  can be expressed in terms of the ones already calculated through  $\beta_{2\parallel} = 2r/(\sigma A_2 \chi_1^2)$ . Some algebra then allows to determine that Stage 1 is firehose unstable, if

$$\sigma < 1 - \frac{4}{\chi_1^2 + 3} - \frac{1}{\chi_1^2}. \tag{15}$$

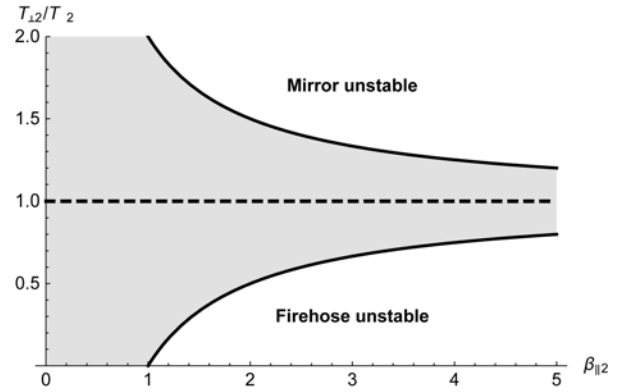


Fig. 2. The stability diagram formed by the mirror and the firehose instabilities. The plasma is stable in the gray region.

As expected, Stage 1 is unstable at low magnetization, for the field is not strong enough to stabilize the anisotropy. In such a case, the plasma will move to the firehose threshold. We now compute the corresponding density jump.

**Stage 2 density jump**

In order to compute the jump when the downstream plasma has to move to the firehose threshold, we need to impose the stability condition (13) into the jump equations (6)–(8). We thus come back to  $U_2 = (P_{2x} + 2n_2 k_B T_{2y})/2n_2$ , still valid since it relies on the necessary equality of temperatures perpendicular to the field in a Vlasov plasma. Then,  $T_{2y}$  is expressed in terms of the field by imposing the stability condition (13). The result for the internal energy  $U_2$  is

$$U_2 = \frac{2P_{2x} - 2B_1^2/8\pi}{2n_2}. \tag{16}$$

Note that the field entering this expression is simply  $B_1$  since it does not change at the front. We can then implement the algorithm used to compute the jump (10). We now find a second-order equation for  $r$ ,

$$r^2 \left(1 + \frac{5}{\chi_1^2}\right) - r \left(5 + \frac{5}{\chi_1^2} - \sigma\right) + 4 = 0, \tag{17}$$

with solutions,

$$r^{\pm} = \frac{5 + \chi_1^2 \left(5 - \sigma \pm \sqrt{\Delta}\right)}{2(5 + \chi_1^2)}, \tag{18}$$

$$\Delta = \frac{25}{\chi_1^4} - \frac{10(\sigma + 3)}{\chi_1^2} + (\sigma - 9)(\sigma - 1). \tag{19}$$

The physical branch must make the junction with the unmagnetized shock jump for  $\sigma = 0$ . It is easily checked that this is  $r^+$ . Yet, beyond a certain  $\sigma$ ,  $r^+$  becomes imaginary because of the square root. But, the solution remains real at least until Stage 1 is found stable.

Figure 6(left) pictures the density jump derived in this section. At low  $\sigma$ , Stage 1 is unstable and the jump is the Stage 2 jump,

given by Eq. (18). As  $\sigma$  increases, it reaches a point where it can stabilize Stage 1, although Stage 2 keeps offering physical solutions (this is quite clear for the case  $\chi_1 = \sqrt{3}$ ). In such a case, the physical solution of our model is Stage 1, Eq. (10), since it is the first stage of the plasma kinetic history, and that it is stable. This is why part of the jump curves for Stage 2, i.e. low  $\sigma$ , are in the short-dashed line within these  $\sigma$ -windows and then comes a  $\sigma$  region where Stage 1 is stable, while Stage 2 no longer offers physical solutions. Obviously in that case, the jump is the one of Stage 1.

The horizontal dashed lines in Figure 6 show the MHD prescriptions. We witness a striking departure from MHD.

**Perpendicular case**

*MHD results*

We now turn to the case where the field is perpendicular to the flow. In contrast with the parallel case, there is now a strong influence of the field at the MHD level. Let us then start reminding the MHD results. The MHD jump equations read (Kulsrud, 2005)

$$n_1 V_1 = n_2 V_2, \tag{20}$$

$$V_1 B_1 = V_2 B_2, \tag{21}$$

$$n_1 V_1^2 + P_1 + \frac{B_1^2}{8\pi} = n_2 V_2^2 + P_2 + \frac{B_2^2}{8\pi}, \tag{22}$$

$$\frac{V_1^2}{2} + \frac{P_1}{n_1} + U_1 + \frac{B_1^2}{4\pi n_1} = \frac{V_2^2}{2} + U_2 + \frac{P_2}{n_2} + \frac{B_2^2}{4\pi n_2}, \tag{23}$$

They can be solved for  $n_2$  following a method similar to the parallel case. We first eliminate  $V_2$  and  $B_2$  thanks to Eqs. (20) and (21). We then express  $P_2$  from Eqs. (22) and (23), and equate the two expressions to find a third-degree polynomial in  $n_2$ . Once factored by  $(r - 1)$ , the positive root of the remaining second-order equation reads

$$r = \frac{\gamma \mathcal{M}_1^2 + \mathcal{M}_{A1}^2 (2 + (\gamma - 1) \mathcal{M}_1^2) - \sqrt{\Delta}}{2(\gamma - 2) \mathcal{M}_1^2}, \tag{24}$$

$$\Delta = 4(\gamma - \gamma^2 + 2) \mathcal{M}_1^4 \mathcal{M}_{A1}^2 + [\gamma \mathcal{M}_1^2 + \mathcal{M}_{A1}^2 (2 + (\gamma - 1) \mathcal{M}_1^2)]^2,$$

where  $\mathcal{M}_1^2 = n_1 V_1^2 / \gamma P_1$  and  $\mathcal{M}_{A1} = V_1 / V_A$ , with  $V_{A1}^2 = n_1 V_1^2 / B_1^2 / 4\pi$ , the upstream Alfvén speed.

We have  $r > 1$ , for

$$\mathcal{M}_1^2 > \frac{\mathcal{M}_{A1}^2}{\sqrt{\mathcal{M}_{A1}^2 - 1}}. \tag{25}$$

For the present study, it is useful to express the limit above in terms of the parameters  $(\sigma, \chi_1)$  defined by Eqs. (1) and (3). The correspondence with the Mach numbers is

$$\sigma = \frac{1}{\mathcal{M}_{A1}^2}, \quad \chi_1^2 = \gamma \mathcal{M}_1^2. \tag{26}$$

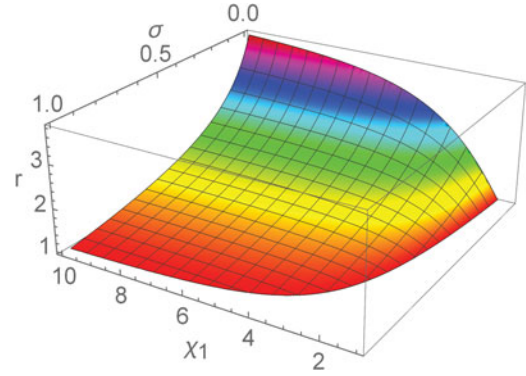


**Fig. 3.** MHD density jump in terms of  $(\sigma, \chi_1)$  for the perpendicular case over the domain  $r > 1$  defined by Eq. (27). In contrast with the MHD parallel case, the field has a strong effect on the shock. We set  $\gamma = 5/3$ .

The result is

$$r > 1 \Leftrightarrow \sigma < \frac{\chi_1^2 - \gamma}{\chi_1^2}. \tag{27}$$

In contrast with the MHD parallel case, a perpendicular field deeply influences the MHD density jump and can even quench the shock. Figure 3 plots the density jump (24) over the domain defined by (27). We now turn to the characterization of Stages 1 and 2.

**Stage 1 density jump and anisotropy**

Stage 1 for the present perpendicular case is analyzed similarly to the parallel case replacing  $P_2$  by  $P_{2x}$  in the jump equations (20)–(23). The jump found that imposing conservation of  $T_{\perp}$  is now

$$r = \frac{3\chi_1^2}{4 + \chi_1^2(1 + 2\sigma)}. \tag{28}$$

It is lower than 1 for

$$\sigma > \frac{\chi_1^2 - 2}{\chi_1^2} \quad \text{or} \quad \chi_1^2 < \frac{2}{1 - \sigma}, \tag{29}$$

so that the model makes physical sense only for  $\chi_1 > \sqrt{2}$ . The anisotropy, computed like in the parallel case, is now,

$$A_2 = \frac{1}{r} + \frac{\chi_1^2}{2r^2} [r(\sigma + 2) - \sigma r^3 - 2]. \tag{30}$$

Plotting  $A_2$  (not shown) in terms of  $(\chi_1, \sigma)$  shows that  $A_2 > 1$  as long as  $r > 1$ . Here, the downstream can therefore be mirror unstable.

**Stage 1 stability**

The stability threshold for the mirror instability is  $A_2 = 1 + 1/\beta_{2\parallel}$  [see Eq. (14)] with now

$$A_2 = \frac{T_{2\perp}}{T_{2\parallel}} = \frac{T_{2x,z}}{T_{2y}} \quad \text{and} \quad \beta_{2\parallel} = \frac{n_2 T_{2\parallel}}{B_2^2 / 8\pi} = \frac{n_2 T_{2y}}{B_2^2 / 8\pi}. \tag{31}$$

Following the method used for the parallel case, we find the threshold for mirror stability of Stage 1 is defined by

$$a_0 + a_1 \sigma + a_2 \sigma^2 + a_3 \sigma^3 = 0, \tag{32}$$

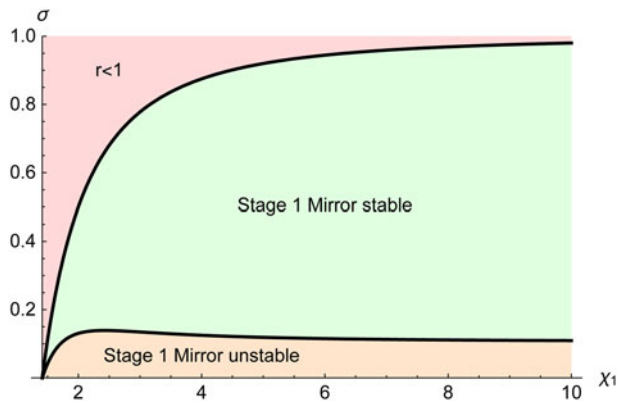


Fig. 4. Numerical analysis of the stability condition (32). Stage 1 is stable inside the green region.

with

$$\begin{aligned}
 a_0 &= 4(\chi_1^2 - 2)(\chi_1^2 + 1)(\chi_1^2 + 4), \\
 a_1 &= -3\chi_1^2(13\chi_1^4 - 4\chi_1^2 + 16), \\
 a_2 &= 12\chi_1^4(\chi_1^2 - 2), \\
 a_3 &= -4\chi_1^6.
 \end{aligned}
 \tag{33}$$

This third-degree polynomial can be analyzed numerically. The result is displayed on Figure 4. Stage 1 is stable inside the green region. The upper red region pictures Eq. (29) beyond which the density jump is lower than unity. Here again, we find that strong enough a field can stabilize Stage 1.

### Stage 2 density jump

In case the field is too weak, the point representing the system in Figure 4 may lie in the lower orange region, with the consequence that it will move to the mirror threshold. We therefore impose  $A_2 = 1 + 1/\beta_{2\parallel}$  in the jump equations and solve them for  $n_2$ . The method is the same than that used for Stage 2 in the parallel case.

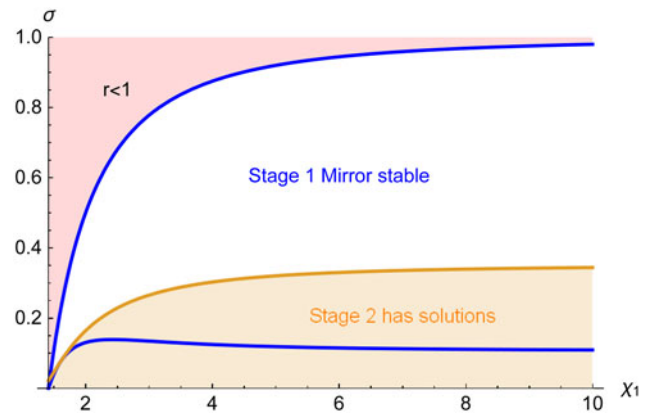


Fig. 5. Stage 2 offers solutions in the orange region. Stage 1 is mirror stable between the two blue lines. If Stage 2 has solutions, while Stage 1 is stable, the downstream settles in Stage 1 since it is the first stage of its kinetic history.

The expression for  $U_2$  to be inserted into these equations is now

$$U_2 = \frac{1}{2} \left( k_B T_{2x} - \frac{B_2^2/8\pi}{n_2} + 2k_B T_{2x} \right) = \frac{1}{2n_2} \left( 3P_{2x} - \frac{B_2^2}{8\pi} \right). \tag{34}$$

The density jump  $r$  is then given by the solution of

$$\begin{aligned}
 2\chi_1^2 \sim r^3 + \left( \frac{10}{\sigma} + \frac{2\chi_1^2}{\sigma} - 4\chi_1^2 \right) \sim r^2 - \left( \frac{10}{\sigma} + \frac{10\chi_1^2}{\sigma} + 5\chi_1^2 \right) r + \frac{8\chi_1^2}{\sigma} \\
 = 0.
 \end{aligned}
 \tag{35}$$

This polynomial has one negative root and two positive ones. Out of these two positive ones, only the largest is physical, as it merges with the MHD jump for  $\sigma = 0$ . For some combinations of  $(\chi_1, \sigma)$ , these two positive roots become imaginary: there, Stage 2 does not offer physical solutions.

Numerical resolution allows to draw Figure 5 where Stage 2 has solutions. Stage 1 is mirror stable between the two blue lines, whereas Stage 2 offers solutions in the orange region. As was the case for the parallel shock, there is a parameter range

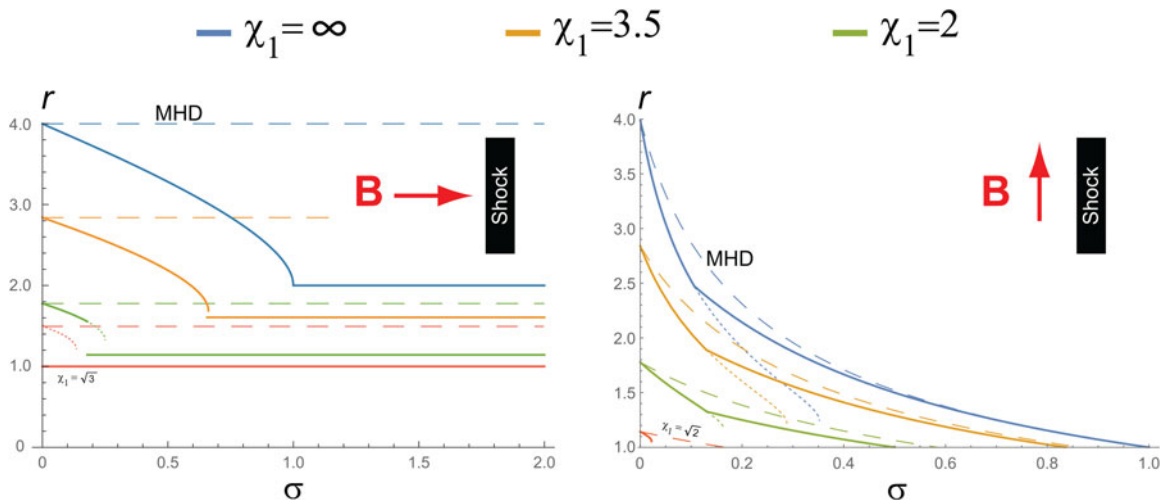


Fig. 6. Density jump for the parallel (left) and the perpendicular cases (right). The long-dashed lines show the MHD predictions. The short-dashed lines show the jump given by Stage 2 when Stage 1 is stable. In such cases, the physical solution is Stage 1 since this is the first stage of the kinetic history of the downstream.

where Stage 1 is stable, while Stage 2 has solutions. In such cases, the system will settle in Stage 1, as it is the first stage of its kinetic history.

Solving Eq. (35) allows to derive the density jump when Stage 2 has solutions, that is, for weak field. The result is plotted in Figure 6(right). The departure from MHD is less pronounced than in the parallel case, because the MHD jump already goes to 0 with increasing fields.

## Conclusion

We studied the departure from MHD jump conditions for magnetized collisionless shocks in non-relativistic pair plasmas. The parallel and perpendicular cases have been assessed. The departure from MHD comes from a downstream anisotropy that can be stably sustained by a magnetic field in a Vlasov plasma. Computing the jump is therefore tantamount to computing the anisotropy. Since the Vlasov equation does not pinpoint any specific anisotropy, but only provides a stable anisotropy window instead, we resort to a hypothesis on the kinetic history of the plasma at the front crossing. We make the partial use of the double adiabatic approximation (Chew *et al.*, 1956) to assume that the temperature  $T_{\perp}$  perpendicular to the motion is conserved from the upstream to the downstream. The excess entropy generated is supposed to go in the directions that are not locked to  $T_{\perp}$  by the field. This stage, called “Stage 1”, can be stable or unstable. If stable, then this is the end stage of the downstream. If unstable, it migrates to “Stage 2” on the nearest instability threshold.

At the low field, Stage 1 is always unstable, as the field is too weak to stabilize the corresponding anisotropy. In the parallel case, it is firehose unstable. In the perpendicular case, it is mirror unstable. In such a case, the downstream moves to the firehose threshold in the parallel case and to the mirror threshold in the perpendicular case. At any rate, the conservation equations fully determine the state of the plasma, so that there is no need to study the pathway to these thresholds. With increasing field amplitude, Stage 1 is eventually stabilized.

Our model makes physical sense only for  $\chi_1 > \sqrt{3}$  in the parallel case, and  $\chi_1 > \sqrt{2}$  in the perpendicular one. If a Mach number is defined like  $\mathcal{M}_1^2 n_1 V_1^2 / \gamma P_1$ , then the present model is physical for  $\mathcal{M}_1 > \sqrt{3/\gamma}$  in the parallel case and  $\mathcal{M}_1 > \sqrt{2/\gamma}$  in the perpendicular one (1.34 and 1.1, respectively, for  $\gamma = 5/3$ ).

The model exhibits a departure from MHD far stronger for the parallel case than for the perpendicular one. This can be related to the ability of a parallel field to guide the particles in the downstream during and after shock formation (Bret *et al.*, 2013a, 2013b; Bret *et al.*, 2014; Stockem Novo *et al.*, 2015; Bret *et al.*, 2016), preventing isotropization, while there is no influence of the field in MHD. In the perpendicular case, even the MHD formalism gives a prominent role to the field so that departure is far less pronounced.

What about oblique shocks? Their analyses are far more involved, as there can be up to three kinds of MHD shocks in this case. This will be the topic of future works.

**Acknowledgments.** A.B. acknowledges support from Grants ENE2016-75703-R from the Spanish Ministerio de Economía y Competitividad and SBPLY/17/180501/000264 from the Junta de Comunidades de Castilla-La Mancha. R.N. was supported by Grants OISE-1743747 and AST-1816420 from the National Science Foundation (NSF). A.B. thanks the Black Hole Initiative (BHI) at Harvard University for hospitality, and R.N. thanks the BHI for support. The BHI is funded by a grant from the John Templeton Foundation.

## References

- Bale SD, Mozer FS and Horbury TS (2003) Density-transition scale at quasi-perpendicular collisionless shocks. *Physical Review Letters* **91**, 265004.
- Bale SD, Kasper JC, Howes GG, Quataert E, Salem C and Sundkvist D (2009) Magnetic fluctuation power near proton temperature anisotropy instability thresholds in the solar wind. *Physical Review Letters* **103**, 211101.
- Bret A (2016) Particles trajectories in Weibel magnetic filaments with a flow-aligned magnetic field. *Journal of Plasma Physics* **82**, 905820403.
- Bret A and Narayan R (2018) Density jump as a function of magnetic field strength for parallel collisionless shocks in pair plasmas. *Journal of Plasma Physics* **84**, 905840604.
- Bret A, Stockem A, Fiúza F, Pérez Álvaro E, Ruyer C, Narayan R and Silva LO (2013a) The formation of a collisionless shock. *Laser and Particle Beams* **31**, 487–491.
- Bret A, Stockem A, Fiúza F, Ruyer C, Gremillet L, Narayan R and Silva LO (2013b) Collisionless shock formation, spontaneous electromagnetic fluctuations, and streaming instabilities. *Physics of Plasmas* **20**, 042102.
- Bret A, Stockem A, Narayan R and Silva LO (2014) Collisionless Weibel shocks: full formation mechanism and timing. *Physics of Plasmas* **21**, 072301.
- Bret A, Stockem Novo A, Narayan R, Ruyer C, Dieckmann ME and Silva LO (2016) Theory of the formation of a collisionless Weibel shock: pair vs. electron/proton plasmas. *Laser and Particle Beams* **34**, 362–367.
- Bret A, Pe’er A, Sironi L, Dieckmann ME and Narayan R (2017a) Departure from MHD prescriptions in shock formation over a guiding magnetic field. *Laser and Particle Beams* **35**, 513–519.
- Bret A, Pe’er A, Sironi L, Sądowski A and Narayan R (2017b) Kinetic inhibition of magnetohydrodynamics shocks in the vicinity of a parallel magnetic field. *Journal of Plasma Physics* **83**, 715830201.
- Chew GF, Goldberger ML and Low FE (1956) The Boltzmann equation and the one-fluid hydromagnetic equations in the absence of particle collisions. *Proceedings of the Royal Society of London A: Mathematical, Physical and Engineering Sciences* **236**, 112–118.
- Feynman R, Leighton R and Sands M (1963) *The Feynman Lectures on Physics*. The Feynman Lectures on Physics No. 2. Reading, Massachusetts: Pearson/Addison-Wesley.
- Gary S (1993) *Theory of Space Plasma Microinstabilities*. Cambridge Atmospheric and Space Science Series. Cambridge: Cambridge University Press.
- Gary SP and Karimabadi H (2009) Fluctuations in electron-positron plasmas: linear theory and implications for turbulence. *Physics of Plasmas* **16**, 042104.
- Gerbig D and Schlickeiser R (2011) Jump conditions for relativistic magnetohydrodynamic shocks in a gyrotropic plasma. *The Astrophysical Journal* **733**, 32.
- Guo X, Sironi L and Narayan R (2017) Electron heating in low-Mach-number perpendicular shocks. I. Heating mechanism. *The Astrophysical Journal* **851**, 134.
- Guo X, Sironi L and Narayan R (2018) Electron heating in low Mach number perpendicular shocks. II. Dependence on the pre-shock conditions. *The Astrophysical Journal* **858**, 95.
- Karimabadi H, Krauss-Varban D and Omid N (1995) Temperature anisotropy effects and the generation of anomalous slow shocks. *Geophysical Research Letters* **22**, 2689–2692.
- Kulsrud RM (2005) *Plasma Physics for Astrophysics*. Princeton, NJ: Princeton University Press.
- Landau LD and Lifshitz EM (1981) *Course of Theoretical Physics, Physical Kinetics*, vol. 10 Oxford: Elsevier.
- Lichnerowicz A (1976) Shock waves in relativistic magnetohydrodynamics under general assumptions. *Journal of Mathematical Physics* **17**, 2135–2142.
- Maruca BA, Kasper JC and Bale SD (2011) What are the relative roles of heating and cooling in generating solar wind temperature anisotropies? *Physical Review Letters* **107**, 201101.
- Miceli M, Orlando S, Burrows DN, Frank KA, Argiroffi C, Reale F, Peres G, Petruk O and Bocchino F (2019) Collisionless shock heating of heavy ions in SN 1987A. *Nature Astronomy* **3**, 236–241.
- Niemiec J, Pohl M, Bret A and Wieland V (2012) Nonrelativistic parallel shocks in unmagnetized and weakly magnetized plasmas. *The Astrophysical Journal* **759**, 73.
- Plotnikov I, Grassi A and Grech M (2018) Perpendicular relativistic shocks in magnetized pair plasma. *Monthly Notices of the Royal Astronomical Society* **477**, 5238–5260.

- Sagdeev RZ** (1966) Cooperative phenomena and shock waves in collisionless plasmas. *Reviews of Plasma Physics* **4**, 23.
- Schlickeiser R, Michno MJ, Ibscher D, Lazar M and Skoda T** (2011) Modified temperature-anisotropy instability thresholds in the solar wind. *Physical Review Letters* **107**, 201102.
- Schwartz SJ, Henley E, Mitchell J and Krasnoselskikh V** (2011) Electron temperature gradient scale at collisionless shocks. *Physical Review Letters* **107**, 215002.
- Sironi L and Spitkovsky A** (2009) Particle acceleration in relativistic magnetized collisionless pair shocks: dependence of shock acceleration on magnetic obliquity. *The Astrophysical Journal* **698**, 1523–1549.
- Stockem Novo A, Bret A, Fonseca RA and Silva LO** (2015) Shock formation in electron-ion plasmas: mechanism and timing. *Astrophysical Journal Letters* **803**, L29.
- Tidman DA** (1967) Turbulent shock waves in plasmas. *Physics of Fluids* **10**, 547–564.
- Vogl DE, Biernat HK, Erkaev NV, Farrugia CJ and Mühlbacher S** (2001) Jump conditions for pressure anisotropy and comparison with the earth's bow shock. *Nonlinear Processes in Geophysics* **8**, 167–174.
- Zel'dovich I and Raizer Y** (2002) *Physics of Shock Waves and High-Temperature Hydrodynamic Phenomena*. Dover Books on Physics. Mineola, New York: Dover Publications.